Ternary Alloys

Volume 21

MSI
Science Simplified

Ternary Alloys

A Comprehensive Compendium of Evaluated Constitutional Data and Phase Diagrams

critically evaluated by MSIT®

Volume 21

Selected Al-Fe-X Ternary Systems for Industrial Applications

Editors
Frank Stein, Martin Palm

Associate Editors
Liya Dreval, Oleksandr Dovbenko, Svitlana Iljenko

Authors
Materials Science International Team, MSIT®

MSI
Science Simplified

Editors: Frank Stein,
Martin Palm
Associate Editors: Liya Dreval
Oleksandr Dovbenko
Svitlana Iljenko

ISBN 978-3-932120-51-0

Vol. 21. Selected Al-Fe-X Ternary Systems for Industrial Applications. – 2022

This volume is part of the book series:
Ternary Alloys: A Comprehensive Compendium of Evaluated Constitutional Data and Phase Diagrams/
Materials Science International Services GmbH, Stuttgart, Germany

Group ISBN for the Ternary Alloys book series: 978-3-932120-41-1

Published by
MSI, Materials Science International Services GmbH, Stuttgart (Federal Republic of Germany)
Am Wallgraben 100, D-70565 Stuttgart, Germany
Postfach 800749, D-70507, Stuttgart, Germany
http://www.msiport.com
http://www.msi-eureka.com/

This book is subject to copyright. All rights reserved (including those of translation into other languages). No part of this book may be reproduced in any form – by photoprint, or any other means – nor transmitted or translated into a machine readable format without written permission from the copyright owner. Registered names, trademarks, etc. used in this book, even when not specifically marked as such, are not to be considered unprotected by law.

© Materials Science International Services GmbH, D-70565 Stuttgart (Federal Republic of Germany), 2022

This book was carefully produced. Nevertheless, authors, editors and publisher do not warrant the information contained therein to be free of errors. Readers are advised to keep in mind that statements, data, illustrations, procedural details or other items may inadvertently be inaccurate.

Printed on acid-free paper.

Printing and binding:
WIRmachenDRUCK GmbH, Mühlbachstraße 7, 71522 Backnang

Printed in the Federal Republic of Germany

Authors: Materials Science International Team, MSIT®

This volume results from collaborative evaluation programs performed by MSI and authored by MSIT®. In this program, data and knowledge are contributed by many individuals and have accumulated over almost thirty five years, up to the present day. The content of this volume is a subset of the ongoing MSIT® Evaluation Programs. Authors of this volume are:

Nataliya Bochvar, Moscow, Russia
Anatoliy Bondar, Kyiv, Ukraine
Gabriele Cacciamani, Genova, Italy
Lesley Cornish, Johannesburg, South Africa
Oleksandr Dovbenko, Stuttgart, Germany
Liya Dreval, Stuttgart, Germany
Yong Du, Changsha, China
Kiyaasha Dyal Ukabhai, Johannesburg, South Africa
Olga Fabrichnaya, Freiberg, Germany
Lorenzo Fenocchio, Genova, Italy
Sergio Gama, Campinas, Brasil
Gautam Ghosh, Evanston, USA
Bernd Grieb, Tübingen, Germany
Kiyohito Ishida, Sendai, Japan
Hermann A. Jehn, Stuttgart, Germany
Kostyantyn Korniyenko, Kyiv, Ukraine
Mario J. Kriegel, Freiberg, Germany
Ortrud Kubaschewski†, Aachen, Germany
K.C. Hari Kumar, Chennai, India
Bernard Legendre, Paris, France
Xiaojing Li, Changsha, China
Shuhong Liu, Changsha, China
Xing Jun Liu, Sendai, Japan
Annelies Malfliet, Heverlee, Belgium
Niraja Moharana, Chennai, India
Martin Palm, Düsseldorf, Germany
Jian Peng, Wuhan, China
Pierre Perrot, Lille, France
Alexander Pisch, Grenoble, France
Qingsheng Ran, Stuttgart, Germany
Maximilian Rank, Karlsruhe, Germany
Peter Rogl, Vienna, Austria
Lazar Rokhlin, Moscow, Russia
Rainer Schmid-Fetzer, Clausthal-Zellerfeld, Germany
Frank Stein, Düsseldorf, Germany
Vasyl Tomashyk, Kyiv, Ukraine
Lyudmila Tretyachenko†, Kyiv, Ukraine
Mikhail Turchanin, Kramatorsk, Ukraine
Oksana Tymoshenko, Kyiv, Ukraine
Thomas Vaubois, Chatillon, France
Alexander Walnsch, Freiberg, Germany
Chuanbin Wang, Wuhan, China
Cui Ping Wang, Sendai, Japan
Junjun Wang, Wuhan, China
Andrew Watson, Chesterfield, UK
Liming Zhang, München, Germany

Contents

Ternary Alloys
A Comprehensive Compendium of Evaluated Constitutional Data and Phase Diagrams

Volume 21
Selected Al-Fe-X Ternary Systems for Industrial Applications

Aluminium – Iron – Phosphorus

Rainer Schmid-Fetzer, updated by Vasyl Tomashyk and Liya Dreval

Introduction

Critical assessments of the Al-Fe-P ternary system have been published by [1988Rag] and [1989Rag], where only three works ([1952Vog, 1965Kan1, 1965Kan2]) were included. The MSIT assessment of the Al-Fe-P system [2007Sch] has covered the literature until the year 2006. Later this system has been thermodynamically optimized in the full compositional range using the CALPHAD method by [2020You1] and through thermodynamic description applying the experimental thermodynamic and phase equilibrium data of the literature by [2015Mie]. The earlier assessment of [2015Mie] was simplified by neglecting order-disorder in the (αδFe) phase.

Information on Al-Fe-P phase relations appeared for the first time in the work of [1952Vog], where the phase equilibria of the Fe-Fe_2P-AlP-$Fe_{50}Al_{50}$ subsystem were studied. There was found that the AlP-Fe_2P section is of the simple eutectic type. The FeAl-AlP section was also presented as quasibinary eutectic section. But the authors explicitly mentioned in the text that this was simplified presentation of the phase equilibria along the FeAl-AlP plane. The liquidus surface, isothermal section and some temperature-compositions sections of the investigated part of this ternary system were constructed also by [1952Vog]. According to the constructed liquidus surface, there should be a maximum in the L ⇌ Fe_2Al_5 + AlP monovariant line. The data of [1952Vog] agree with one of [1965Kan1]. This system was also optimized by [2015Mie] and [2020You1] in full concentration range and some isothermal and vertical sections were constructed using the thermodynamic calculations.

The solubility of P in αFe containing Al was investigated by [1965Kan2] and [2020You1].

Some thermodynamic properties of the Al-Fe-P alloys were investigated by [1979Yam, 1983Ban, 1983Yam, 1993Din] and amorphous phase formation in this system was discussed in [1983Ino].

Investigations of the system are listed in Table 1.

Binary Systems

Binary Al-P and Fe-P systems are accepted from [2020You2]. The Al-Fe phase diagram is accepted from the binary evaluation report of [2022Ste] and presented in the chapter "*Al - Fe (Aluminium - Iron)*" of this volume.

Solid Phases

No ternary compounds were found in the Al-Fe-P system. All unary and binary phases are listed in Table 2. Solubility of P in αFe, containing 1 at.% Al, increases linearly from about 0.7 at.% at 650°C to about 4 at.% at 1050°C and decreases from 4.4 at.% in pure αFe to 2.1 at.% at 7.9 at.% Al at 1000°C [1965Kan2]. The solubility of P in ferrite Al-Fe alloys decreases from 2.28 to 1 mass% (3.1 to 1.47 at.%) with the added Al increases up to 5 mass% (9.6 at.%) [2020You1]. The maximum solubility of Fe in AlP, P in FeAl and Al in Fe_3P and Fe_2P are 2.7, 1.8, 2.1 and 1.7 at.%, respectively [2012Wu, 2013Rag].

The site occupation behavior of phosphorus in the binary FeAl alloy was investigated by a thermodynamics model combining with first-principles calculations [2012Li]. The results obtained show that P atoms occupy exclusively the Al sites.

Quasibinary Systems

According to the data [1952Vog], the AlP-Fe_2P section forms a simple eutectic quasibinary system. The section itself was not presented in the original paper. Therefore, it could not be reproduced here. The eutectic reported at 1225°C by [1952Vog] is given as e_2, maximum in Table 3.

Invariant Equilibria

The data of [1952Vog], the results of the thermodynamic assessment [2020You1] and information about the accepted binary systems were used to construct the reaction scheme of the system. Only invariant reactions involving the liquid phase were included. It should be noted that [2020You1] incorrectly labeled some phases in table 5 of their original work. The authors did not provide the composition of solid phases participating in the invariant and information on the maxima occurring in some of the calculated monovariant lines. The results of [2020You1] were accepted here with modifications since this is the only work presenting the invariant reactions in the whole composition range.

Certain changes were introduced to preserve agreement with the available quantitative data of [1952Vog] and the binary Al-Fe system accepted in the present work. [1988Rag, 1989Rag] also proposed their partial reaction schemes which are mainly based on the experimental data of [1952Vog]. [2015Mie] also calculated the invariant equilibria in the region below 70 at.% P.

[1952Vog] presented experimental results for the iron corner of the concentration triangle and for narrow composition region between 0 to 10 at.% P along the $Fe_{50}Al_{50}$-AlP section. In this composition region, we tried to preserve the agreement with the available experimental data set as close as possible. For the higher Al and P concentrations, [1952Vog] reported significant difficulties in accurate establishing of the phase equilibria and did not propose any quantitative data. Therefore, the calculation results of [2020You1] were used as a basis to construct the reaction scheme in the Al and P corners.

According to the calculations of [2020You1], a number of four-phase invariant reactions and invariant maxima appear in the system. However, the experimental evidences are available only for some of them. These are the e_2 eutectic in the AlP-Fe_2P quasibinary section, e_6 (maximum), U_6, and E_2 reactions (Fig. 1). [2020You1] did not mention the e_2 and e_6 maxima in the L + AlP + Fe_2P and L + FeAl + AlP monovariant line in their paper. But these invariant reactions should appear in the corresponding curves judging from the shape of the liquidus surface, their adjacent invariant reactions and vertical sections presented in the original paper. The temperatures of the e_2, U_6, and E_3 reactions were accepted according to the experimental data of [1952Vog] (Table 3). According to [1952Vog], the e_6 maximum should appear at 1125°C while, according to the calculations of [2020You1], it is located at around 1101°C (as read from the original figure). The results of [2020You1] were accepted here for the e_6 maximum to preserve the consistency with the calculated liquidus surface in the Al rich part of the concentration triangle and vertical sections. The e_6 coordinates are only approximate, since [2020You1] did not provid the corresponding calculated data.

There is another point to be discussed in connection with the e_6 maximum. In their original paper, [2020You1] denoted the invariant reaction with the participation of the liquid phase, Fe_5Al_8, FeAl, and AlP as a transition-type reaction. Considering the temperatures of the adjacent e_6, p_1, and U_5 equilibria, this would be possible if a minimum existed in the L + Fe_5Al_8 + AlP or L + Fe_5Al_8 +FeAl monovariant curves. The data provided by [2020You1] were too scarce to justify the occurrence of such minimum and proposed type of the four-phase reaction. Therefore, the invariant reaction involving the liquid phase, Fe_5Al_8, FeAl, and AlP was denoted as E_2 (Table 3) to maintain agreement with the Al-Fe phase diagram and available vertical sections. In the liquidus surface calculated by [2015Mie], the reaction between L, Fe_5Al_8, FeAl, and AlP was also presented as transitional, but the calculated vertical sections did not comprise the composition range with this reaction. Therefore, the result of [2015Mie] could not be justified by the available information.

The current reaction scheme differs from the one suggested by [1952Vog, 1988Rag, 1989Rag] by the incorporation of $FeAl_2$, which appears in the Al rich part of the liquidus. The L + Fe_2Al_5 ⇌ Fe_5Al_8 + $FeAl_2$ reaction of [2020You1] was changed to the Fe_5Al_8 + Fe_2Al_5 ⇌ L + $FeAl_2$ (U_2 at 1142°C) reaction to maintain the agreement with the peritectoid formation of $FeAl_2$ at 1146°C in the binary Al-Fe system accepted in the present work. The e_5 maximum was added in the L + Fe_2Al_5 + AlP monovariant line to preserve the consistency with the adjacent U_3 and U_4 reactions calculated by [2020You1]. This maximum was added following the suggestion of [1952Vog]. However, [1952Vog] provided no experimental evidence supporting the occurrence of such maximum.

In the Al corner, the L + (Al) ⇌ Fe_4Al_{13} + AlP reaction at 1099°C calculated by [2020You1] was replaced by the D_1 reaction at around 652°C. The temperature of "1099°C" given by [2020You1] is most probably a misprint. It is hardly possible that the (Al) phase melting at 660°C could be stabilized up to such high temperature in the Al-Fe-P system.

In the Al rich part, the current reaction scheme differs from the one suggested by [2020You1] by the incorporation of the D_2 reaction and the e_3 maximum. The latter was required to maintain the agreement with the E_1 and U_1 reactions.

The calculations of [2020You1] suggest that at least one solid phase invariant reactions exist in the system. However, the authors provided no data for such type of invariant equilibria.

The temperatures and available compositions are listed in Table 3. The compositions of solid phases are given for the stoichiometric compounds only.

Liquidus Surface

The liquidus surface of the Al-Fe-P system is given in Fig. 1. It is based on the liquidus surface projection calculated by [2020You1], but contains a number of modifications related to the invariant reactions. The changes were already described in the "*Invariant Equilibria*" section. The dashed line denotes the AlP-Fe_2P quasibinary section. The most interesting feature of the liquidus surface projection presented in the current evaluation is the primary crystallization regions for FeAl and $FeAl_2$.

The liquidus surface of this system at phosphorus contents above 30 at.% was also calculated by [2015Mie].

Isothermal Sections

A partial isothermal section in the Fe rich corner at 1000°C is shown in Fig. 3, and the isothermal sections of the Al-Fe-P system at 800°C, 650°C, and 450°C are given in Figs. 4 to 6. These isothermal sections are accepted according to [2020You1] but slightly modified to preserve agreement with the accepted Al-Fe diagram. The phase regions shown with dotted line in Fig. 6 were added in the present work. These regions related to the low-temperature Fe_3Al phase which was not taken into account by [2020You1]. The isothermal sections of this system at 1130°C, 1000°C (only in Fe corner), and 450°C in Cartesian coordinates were constructed by [2015Mie], at 750°C by [2011Che] and at 450°C by [2012Wu, 2013Rag].

Temperature – Composition Sections

The vertical sections at 6 and 9 mass% P and at 10 and 25 mass% Al are shown in Figs. 7 to 10, respectively. They are accepted according to [2020You1] but corrected to maintain the consistency with the reaction scheme and liquidus surface constructed in the present evaluation and to reach better agreement to the experimental data of [1952Vog].

Thermodynamics

Aluminium was found to increase the activity of P in liquid Fe at 1600°C, the interaction coefficients being $\varepsilon^{Al}_P = 4.6 \pm 0.7$ and $\varepsilon^{Al}_P = 0.037$ [1979Yam, 1983Yam] ($\varepsilon^{Al}_P = 3.57 \pm 0.33$ [1983Ban], according to the thermodynamic calculation the value of this coefficients is equal $\varepsilon^{Al}_P = 8.78$ [1993Din]). According to the optimization of the Al-Fe-P ternary system by [2020You1], the activity coefficient interaction parameters were determined as $\varepsilon^{P}_{Al} = 2.878$ at 1600°C and 2.655 at 1400°C.

Miscellaneous

It was found that Al has a weak tendency to combine with P in steel because any phosphide phases except Fe_3P were not found in the Al-Fe-P ternary system [1965Kan1].

Amorphous phase formation with good ductility has been found in this ternary system by using a melt-spinning technique [1983Ino]. Formation of a completely amorphous phase was achieved for a wide range of compositions as shown in Fig. 11 (0 to 18 at.% Al and 13 to 21 at.% P). Crystallization temperature and Vickers hardness increase with increasing Al and P content and maximum values are attained at 448°C and 640 diamond pyramid number for $Al_{16}Fe_{66}P_{18}$ alloy. Their fracture strengths are about 2000 MPa. The activation energy for amorphous phase crystallization is estimated to be about 315 $kJ \cdot mol^{-1}$ for $Al_4Fe_{78}P_{18}$ and 340 $kJ \cdot mol^{-1}$ for $Al_8Fe_{74}P_{18}$ [1983Ino].

Treatments of a pure Al melt at 800°C with the equivalent of 200 to 800 mass ppm P by means of an Al-Fe-P addition prior to casting results in a distribution of polyhedral AlP particles of medium size from ~ 6 to 9 μm with some tendency of cluster formation at the higher levels of addition [2001Kyf].

The mechanical properties of commercial purity Al could be improved after refining in a KCl-NaCl-Na_3AlF_6 flux containing 10 mass% AlP [2011Che].

References

[1952Vog] Vogel, R., Klose, H., “The Iron-Iron Phosphide-Aluminium Phosphide-Aluminium Phase Diagram” (in German), *Arch. Eisenhuettenwes.*, **23**(7-8), 287-291 (1952), doi:10.1002/srin.195200953 (Experimental, Morphology, Phase Diagram, Phase Relations, #, *, 4)

[1958Tay] Taylor A., Jones, R.M., “Constitution and Magnetic Properties of Iron-Rich Iron-Aluminium Alloys”, *J. Phys. Chem. Solids*, **6**, 16-37 (1958), doi:10.1016/0022-3697(58)90213-0 (Crystal Structure, Experimental, Magnetic Properties, Phase Diagram, Phase Relations, 49)

[1965Kan1] Kaneko, H., Nishizawa, T., Tamaki, K., “Phosphide-Phases in Ternary Alloys of Iron, Phosphorus and other Elements” (in Japanese), *Nippon Kinzoku Gakkai-shi*, **29**(2), 159-165 (1965), doi:10.2320/jinstmet1952.29.2_159 (Experimental, Morphology, Phase Diagram, 24)

[1965Kan2] Kaneko, H., Nishizawa, T., Tamaki, K., Tanifuji, A., “Solubility of Phosphorus in α and γ Iron” (in Japanese), *Nippon Kinzoku Gakkai Shi*, **29**(2), 166-170 (1965), doi:10.2320/jinstmet1952.29.2_166 (Experimental, Phase Relations, 20)

[1979Yam] Yamada, K., Kato, E., “Mass Spectrometric Determination of Activities of Phosphorus in Liquid Fe-P-Si, Al, Ti, V, Cr, Co, Ni, Nb and Mo Alloys” (in Japanese), *Tetsu-to-Hagane (J. Iron Steel Inst.*

Jap.), **65**(2), 273-280 (1979), doi:10.2355/tetsutohagane1955.65.2_273 (Experimental, Thermodynamics, 40)

[1983Ban] Ban-ya, S., Maruyama, N., Fujino, S., "The Effect of C, Si, Sn and B on the Activity of Phosphorus in Liquid Iron" (in Japanese), *Tetsu to Hagane*, **69**(8) 921-928 (1983), doi:10.2355/tetsutohagane1955.69.8_921 (Experimental, Thermodynamics, 32)

[1983Ino] Inoue, A., Kitamura, A., Masumoto, T., "The Effect of Aluminium on Mechanical Properties and Thermal Stability of (Fe,Ni)-Al-P Ternary Amorphous Alloys", *J. Mater. Sci.*, **18**, 753-758 (1983), doi:10.1007/BF00745573 (Experimental, Phase Relations, Thermodynamics, #, 11)

[1983Yam] Yamada, K., Kato, E., "Effect of Dilute Concentrations of Si, Al, Ti, V, Cr, Co, Ni, Nb and Mo on the Activity Coefficient of P in Liquid Iron", *Trans. Iron Steel Inst. Jap.*, **23**(1), 51-55 (1983), doi:10.2355/isijinternational1966.23.51 (Experimental, Thermodynamics, 16)

[1988Rag] Raghavan, V., "The Al-Fe-P (Aluminium-Iron-Phosphorus) System", in "*Phase Diagrams of Ternary Iron Alloys*", Indian Inst. Metals, Calcutta, **3**, 9-16 (1988) (Review, Crystal Structure, Phase Diagram, Phase Relations, 5)

[1989Rag] Raghavan, V., "The Al-Fe-P System (Aluminium-Iron-Phosphorus)", *J. Alloy Phase Diagrams*, **5**(1), 32-39 (1989) (Review, Crystal Structure, Phase Diagram, Phase Relations, 5)

[1993Din] Ding, X., Wang, W., Han, Q., "Thermodynamic Calculation of Fe-P-j System Melt" (in Chinese), *Acta Metall. Sin. (China)*, **29**(12), B527-B532 (1993) (Calculation, Theory, Thermodynamics, 7)

[1993Kat] Kattner, U.R., Burton, B.P., "Al-Fe (Aluminum-Iron)" in "*Phase Diagrams of Binary Iron Alloys*", Okamoto, H. (Eds.), Mater. Park OH: ASM Int., 12-28 (1993) (Crystal Structure, Electrical Properties, Magnetic Properties, Mössbauer, Phase Diagram, Phase Relations, Review, Thermodynamics, *, 99)

[1994Bur] Burkhardt, U., Grin, J., Ellner, M., Peters, K., "Structure Refinement of the Iron-Aluminium Phase with the Approximate Composition Fe_2Al_5", *Acta Crystallogr., Sect. B: Struct. Crystallogr. Crys. Chem.*, **B50**, 313-316 (1994), doi:10.1107/S0108768193013989 (Crystal Structure, Experimental, 9)

[2001Kyf] Kyffin, W.J., Rainforth, W.M., Jones, H., "The Formation of Aluminum Phosphide in Aluminum Melt Treated with an Al-Fe-P Inoculant Addition", *Z. Metallkd.*, **92**(4), 396-398 (2001), doi:10.3139/ijmr-2001-0077 (Experimental, Morphology, Phase Relations, 14)

[2007Sch] Schmid-Fetzer, R., Tomashik, V., "Al-Fe-P Ternary Phase Diagram Evaluation", in *MSI Eureka*, Effenberg, G. (Ed.), MSI, Materials Science International Services GmbH, Stuttgart (2007), Document ID: 10.20741.2.7 (Crystal Structure, Phase Diagram, Phase Relations, Assessment, 13)

[2007Ste] Stein, F., Palm, M., "Re-Determination of Transition Temperatures in the Fe-Al System by Differential Thermal Analysis", *Int. J. Mater. Res.* (*Z. Metallkd.*), **98**(7), 580-588 (2007), doi:10.3139/146.101512 (Experimental, Phase Diagram, Phase Relations, *, 59)

[2008Gil] Gille, P., Bauer, B., "Single Crystal Growth of $Al_{13}Co_4$ and $Al_{13}Fe_4$ from Al-Rich Solutions by the Czochralski Method", *Cryst. Res. Technol.*, **43**(11), 1161-1167 (2008), doi:10.1002/crat.200800340 (Crystal Structure, Experimental, Morphology, Phase Relations, Theory, 17)

[2010Chu] Chumak, I., Richter, K.W., Ehrenberg, H., "Redetermination of Iron Dialuminide, $FeAl_2$", *Acta Crystallogr., Sect. C*, **C66**, i87-i88 (2010), doi:10.1107/S0108270110033202 (Experimental, Crystal Structure, 10)

[2010Pop] Popcevic, P., Smontara, A., Ivkov, J., Wencka, M., Komelj, M., Jeglic, P., Vrtnik, S., Bobnar, M., Jaglicic, Z., Bauer, B., Gille, P., Borrmann, H., Burkhardt, U., Grin, Yu., Dolinsek, J., "Anisotropic Physical Properties of the $Al_{13}Fe_4$ Complex Intermetallic and its Ternary Derivative $Al_{13}(Fe,Ni)_4$", *Phys. Rev. B: Condens. Matter*, **81**(18), 184203 (2010), doi:10.1103/PhysRevB.81.184203 (Crystal Structure, Electrical Properties, Experimental, Magnetic Properties, Morphology, Physical Properties, Thermodynamics, Transport Phenomena, 42)

[2010Ste] Stein, F., Vogel, S.C., Eumann, M., Palm, M., "Determination of the Crystal Structure of the ε Phase in the Fe-Al System by High-Temperature Neutron Diffraction", *Intermetallics*, **18**(1), 150-156 (2010), doi:10.1016/j.intermet.2009.07.006 (Crystal Structure, Experimental, Morphology, Phase Relations, 40)

[2011Che] Chen, C., Wang, J., Shu, D., Li, P., Xue, J., Sun, B., "A Novel Method to Remove Iron Impurity from Aluminum", *Mater. Trans.*, **52**(8), 1629-1633 (2011), doi:10.2320/matertrans.M2011108 (Calculation, Crystal Structure, Electrochemistry, Experimental, Kinetics, Morphology, Phase Diagram, Phase Relations, Transport Phenomena, 18)

[2012Li] Li, H., Li, M., Wu, Yi., Zhou, H., Wu, X., Zhu, Zh., Li, Ch., Xu, L., Ji, J., Hua, Y., Su, T., Ji, Ch., Zhang, W., "Site Occupation Behaviour of Sulfur and Phosphorus in NiAl, TiAl and FeAl",

Intermetallics, **28**, 156-163 (2012), doi:10.1016/j.intermet.2012.04.017 (Calculation, Crystal Structure, Thermodynamics, 58)

[2012Wu] Wu, Ch., Huang, W., Su, X., Peng, H., Wang, J., Liu, Ya, "Experimental Investigation and Thermodynamic Calculation of the Al-Fe-P System at Low Phosphorus Contents", *Calphad*, **38**, 1-6 (2012), doi:10.1016/j.calphad.2012.03.005 (Calculation, Crystal Structure, Experimental, Morphology, Phase Diagram, Phase Relations, Thermodynamics, 27)

[2013Rag] Raghavan, V., "Phase Diagram Updates and Evaluations of the Al-Fe-P, B-Fe-U, Bi-Fe-Zn, Cu-Fe-Zn, Fe-Si-Zn and Fe-Ti-V Systems", *J. Phase Equilib. Diffus.*, **34**(3), 230-243 (2013), doi:10.1007/s11669-013-0230-5 (Phase Diagram, Phase Relations, Review, 9)

[2015Mie] Miettinen, J., Louhenkilpi, S., Vassilev, G., "Thermodynamic Description of Ternary Fe-X-P Systems. Part 9: Fe-Al-P", *J. Phase Equilib. Diffus.*, **36**(4), 317-326 (2015), doi:10.1007/s11669-015-0383-5 (Calculation, Thermodynamics, Phase Diagram, Phase Relations, 67)

[2016Li] Li, X., Scherf, A., Heilmaier, M., Stein, F., "The Al-Rich Part of the Fe-Al Phase Diagram", *J. Phase Equilib. Diffus.*, **37**, 162-173 (2016), doi:10.1007/s11669-015-0446-7 (Crystal Structure, Experimental, Phase Diagram, Phase Relations, 38)

[2019Ran] Rank, M., Franke, P., Seifert, H.J., "Thermodynamic Investigations in the Al-Fe System: Thermodynamic Modeling Using Calphad", *Int. J. Mater. Res.*, **110**(5), 406-421 (2019), doi:10.3139/146.111765 (Calculation, Crystal Structure, Phase Diagram, Phase Relations, Thermodynamics, 108)

[2020You1] You, Z., Ju, I.-H., "Critical Evaluation and Thermodynamic Optimization of the Al-P and Fe-Al-P Systems", *J. Phase Equilib. Diffus.*, **41**(5), 598-614 (2020), doi:10.1007/s11669-020-00822-4 (Calculation, Experimental, Phase Diagram, Phase Relations, Review, Thermodynamics, #, 63)

[2020You2] You, Z., Jung, I. H., "Critical Evaluation and Thermodynamic Optimization of the Fe-P System", *Metall. Mater. Trans. B*, **51**(6), 3108-3129 (2020), doi:10.1007/s11663-020-01939-0 (Assessment, Calculation, Phase Diagram, Phase Relations, Thermodynamics, 70)

[2022Ste] Stein, F., "Al-Fe Binary Phase Diagram Evaluation", in *MSI Eureka*, Watson, A. (Ed.), MSI, Materials Science International Services GmbH, Stuttgart (2022), Document ID: 20.10236.2.7 (2022), doi:10.7121/msi-eureka-20.10236.2.7 (Crystal Structure, Phase Diagram, Phase Relations, Assessment, 311)

Table 1: Investigations of the Al-Fe-P Phase Relations, Structures and Thermodynamics

Reference	Method / Experimental Technique	Temperature / Composition / Phase Range Studied
[1952Vog]	DTA, metallography	up to 1500°C / Fe-Fe_2P-AlP-Al
[1965Kan1]	XRD, chemical analysis	800°C / 3.78 at.% Al + 91.75 at.% Fe + 4.47at.% P and 7.51 at.% Al + 88.23 at.% Fe + 4.26 at.% P
[1965Kan2]	DTA, XRD	650-1050°C
[1979Yam], [1983Yam]	Knudsen cell mass spectrometry	1600°C
[1983Ban]	Transportation method	1400°C / Al-Fe-P
[1983Ino]	DTA, DSC, XRD, TEM, Vickers microhardness testing	up to 500°C / Al-Fe-P
[1993Din]	Calculation	1600°C / Al-Fe-P
[2001Kyf]	SEM with EDS	800°C / Al-Fe-P
[2011Che]	Calculation	750°C / Al-Fe-P
[2012Wu]	Metallography, XRD, SEM-EDS	450°C / Al-Fe-P
[2015Mie]	Thermodynamic description	up to 1600°C / Al-Fe-P
[2020You1]	CALPHAD	up to 1600°C / Al-Fe-P

Table 2: Crystallographic Data of Solid Phases

Phase/ Temperature Range (°C)	Pearson Symbol/ Space Group/ Prototype	Lattice Parameters (pm)	Comments/References
(Al) < 660.452	*cF*4 *Fm*$\bar{3}$*m* Cu	*a* = 404.96	pure Al at 25°C [Mas2] solubility for Fe: 0.023 at.% [2019Ran]
(αδFe) < 1540	*cI*2 *Im*$\bar{3}$*m* W		Strukturbericht designation: *A*2 [2007Ste] solubility for Al: 45.0 at.% [1993Kat, 2007Ste]
αFe < 912		*a* = 286.65	at 25°C [Mas2]
δFe 1538 - 1394		*a* = 293.15	[Mas2]
(γFe) 1394 - 912	*cF*4 *Fm*$\bar{3}$*m* Cu	*a* = 364.67	at 915°C [V-C2, Mas2]
(P) (red) < 417	*c**66		sublimation at 1 bar triple point at 576°C, > 36.3 bar, triple point at 589.6 at 1 atm [Mas2]
		a = 1131	[V-C2]
(P) (white) < 44.14	*c*** ? P (white)	*a* = 718	at 25°C [Mas2] common form of elemental P, probably less stable than P (red) at 25°C [Mas2]
(P) (black)	*oC*8 *Cmca* P (black)	*a* = 31.36 *b* = 1047.8 *c* = 437.63	at 25°C [Mas2]
AlP < 2532	*cF*8 *F*$\bar{4}$3*m* ZnS	*a* = 546.25 ± 0.05	[V-C2, Mas2]
Fe_3Al < 545	*cF*16 *Fm*$\bar{3}$*m* BiF_3		sometimes named α_1 phase Strukturbericht designation: $D0_3$ ~24 to ~34 at.% Al at 400°C [1993Kat]
		a = 579.30	at 23.1 at.% Al, water-quenched from 250°C [1958Tay]
		a = 578.86	at 35.0 at.% Al, water-quenched from 250°C [1958Tay]
FeAl < 1318	*cP*2 *Pm*$\bar{3}$*m* CsCl		sometimes named α_2 phase Strukturbericht designation: *B*2 23.5 to ~53 at.% Al [2007Ste]
		a = 289.53 to 290.90	at 36.2-50.0 at.% Al, water-quenched from 250°C [1958Tay]
Fe_5Al_8 1231 - 1095	*cI*52 *I*$\bar{4}$3*m* Cu_5Zn_8		sometimes named ε phase Strukturbericht designation: $D8_2$ 56.0 to 64.5 at.% Al [2016Li]
		a = 897.57 ± 0.02	at 1120°C and 59.4 at.% Al [2010Ste]
$FeAl_2$ < 1146	*aP*19 *P*$\bar{1}$ $FeAl_2$	*a* = 487.45 *b* = 645.45 *c* = 873.61 α = 87.930° β = 74.396° γ = 83.062°	sometimes named ζ phase 64.7 - 66.7 at.% Al at 1000°C [2016Li] at 66.4 at.% Al [2010Chu]

Phase/ Temperature Range (°C)	Pearson Symbol/ Space Group/ Prototype	Lattice Parameters (pm)	Comments/References
Fe_2Al_5	*oC*24		sometimes named η phase
1159 - ~331	*Cmcm*		68.4 to 72.5 at.% Al
	Fe_2Al_5	*a* = 765.59 ± 0.08	at 71.5 at.% Al [1994Bur]
		b = 641.54 ± 0.06	
		c = 421.84 ± 0.04	
Fe_4Al_{13}	*mC*102		referred to as $FeAl_3$ in old literature before
< 1150	*C*2/*m*		~1995
	Fe_4Al_{13}		sometimes named θ phase
			74.5 - ~76.9 at.% Al
		a = 1548.8 ± 0.1	single crystal grown by Czochralski technique
		b = 808.66 ± 0.05	[2008Gil, 2010Pop]
		c = 1247.69 ± 0.08	
		β =(107.669±0.004)°	
Fe_3P	*tI*32	*a* = 910.0	at 22°C
< 1151	$I\bar{4}$	*c* = 445.92	
	Ni_3P	*a* = 913.7	at 414°C
		c = 450.62	
		a = 917.4	at 678°C, mineral Schreibersite
		c = 452.99	[V-C2, Mas2]
Fe_2P	*hP*9	*a* = 586.75 ± 0.02	33.3 to 34 at.% P, mineral Barringerite [V-C2,
< 1374	$P\bar{6}2m$	*c* = 345.81 ± 0.02	Mas2]
	Fe_2P		
FeP	*oP*8	*a* = 519.10	[V-C2, Mas2]
< 1395	*Pmna*	*b* = 309.83	
	MnP	*c* = 579.09	
FeP_2	*oP*6	*a* = 497.29 ± 0.07	66 to 67 at.% P [V-C2, Mas2]
< 1184	*Pnnm*	*b* = 565.68 ± 0.08	
	FeS_2	*c* = 272.30 ± 0.04	

Table 3: Invariant Equilibria

Reaction	*T*(°C)	Type	Phase	Composition (at.%)		
				Al	Fe	P
L ⇌ Fe_2P + AlP	1225	e_2 (max)	L	8.8	54.8	36.4
			Fe_2P	0	67.7	33.3
			AlP	50	0	50
L ⇌ FeP + AlP	> 1208	e_3 (max)	L	6	44	50
			FeP	0	50	50
			AlP	50	0	50
L ⇌FeP + Fe_2P + AlP	1208	E_1	L	54.6	6.1	39.3
			FeP	0	50	50
			AlP	50	0	0
L + FeP ⇌ FeP_2 + AlP	1170	U_1	L	2.8	29.7	67.5
			FeP	0	50	50
			FeP_2	0	66.7	33.3
			AlP	50	0	50
Fe_5Al_8+ Fe_2Al_5 ⇌ L + $FeAl_2$	1142	U_2	L	66.8	32.2	1.0
L ⇌ Fe_2Al_5+ AlP	> 1139	e_5 (max)	L	27.9	70.5	1.6
			AlP	50	0	50
L + Fe_2Al_5 ⇌ Fe_4Al_{13} + AlP	1139	U_3	L	73.7	25.3	1.0
			AlP	50	0	50

Reaction	T(°C)	Type	Phase	Composition (at.%)		
				Al	Fe	P
$L + Fe_2Al_5 \rightleftharpoons FeAl_2 + AlP$	1130	U_4	L	64.6	33.1	2.3
			AlP	50	0	50
$L + FeAl_2 \rightleftharpoons Fe_5Al_8 + AlP$	1118	U_5	L	59.1	37.2	3.7
			AlP	50	0	50
$L \rightleftharpoons FeAl + AlP$	> 1099	e_6 (max)	L	42	51	7
			AlP	50	0	50
$L \rightleftharpoons Fe_5Al_8 + FeAl + AlP$	1099	E_2	L	53.1	41.2	5.7
			AlP	50	0	50
$L + Fe_3P \rightleftharpoons Fe_2P + (\alpha\delta Fe)$	1020	U_6	L	8.9	72.0	19.1
$L + (\alpha\delta Fe) \rightleftharpoons Fe_2P + FeAl$	1015	C_1, critical	L	16.2	65.3	18.5
$L \rightleftharpoons FeAl + AlP + Fe_2P$	995	E_3	L	26.4	54.7	18.9
			AlP	50	0	50
$L \rightleftharpoons (Al) + Fe_4Al_{13} + AlP$	~ 652	D_1	L	99.2	0.7	0.1
			(Al)	100	0	0
			AlP	50	0	50
$L \rightleftharpoons (P) + FeP_2 + AlP$	< 575	D_2	L	0.1	0.8	99.1
			(P)	0	0	100
			AlP	50	0	50

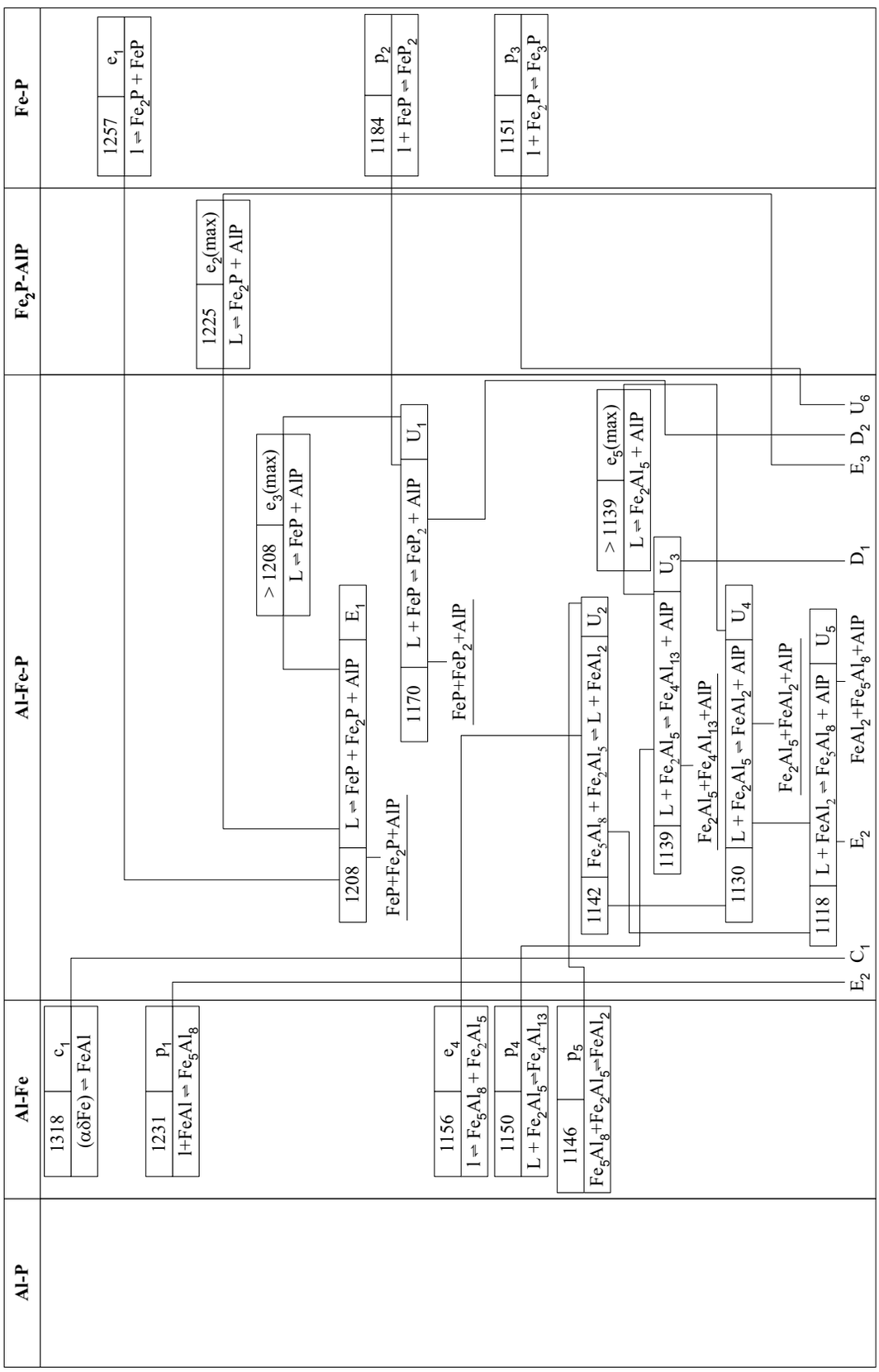

Fig. 1a: Al-Fe-P. Reaction scheme

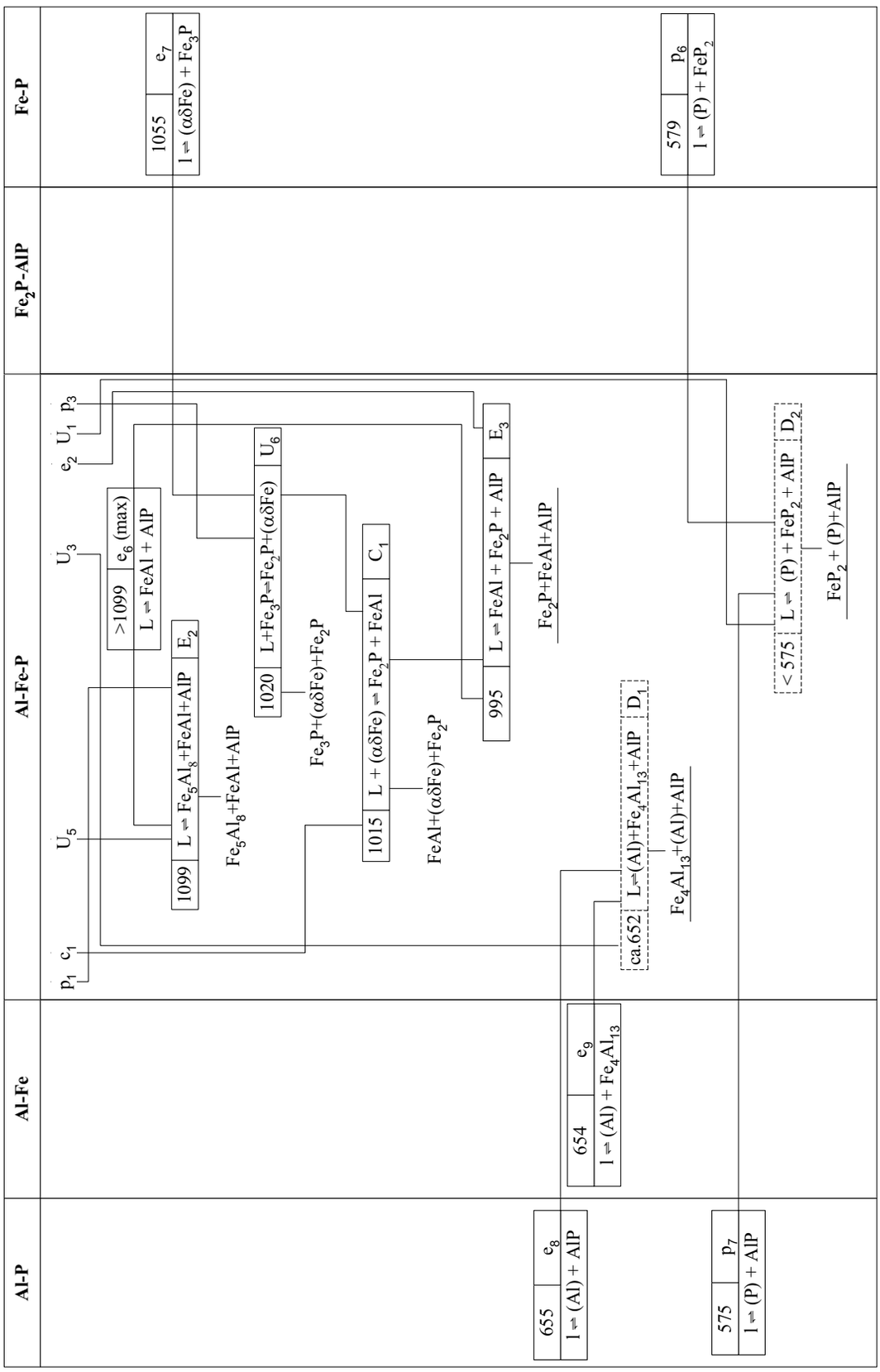

Fig. 1b: Al-Fe-P. Reaction scheme

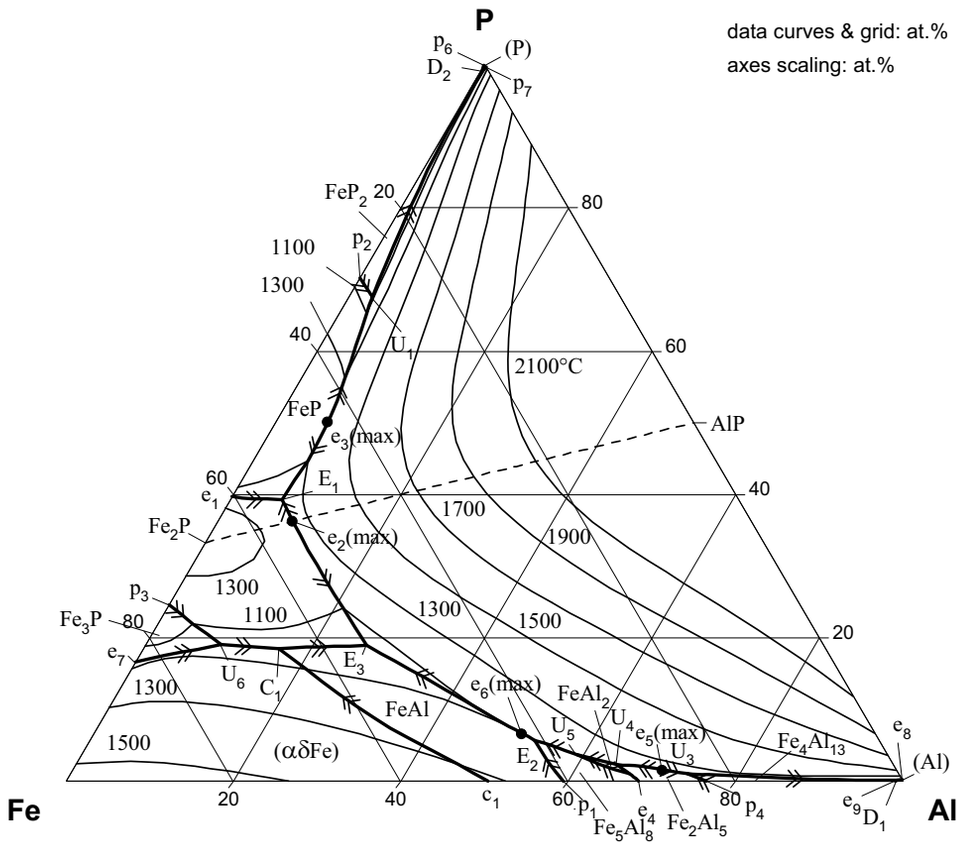

Fig. 2a: Al-Fe-P. Liquidus surface projection

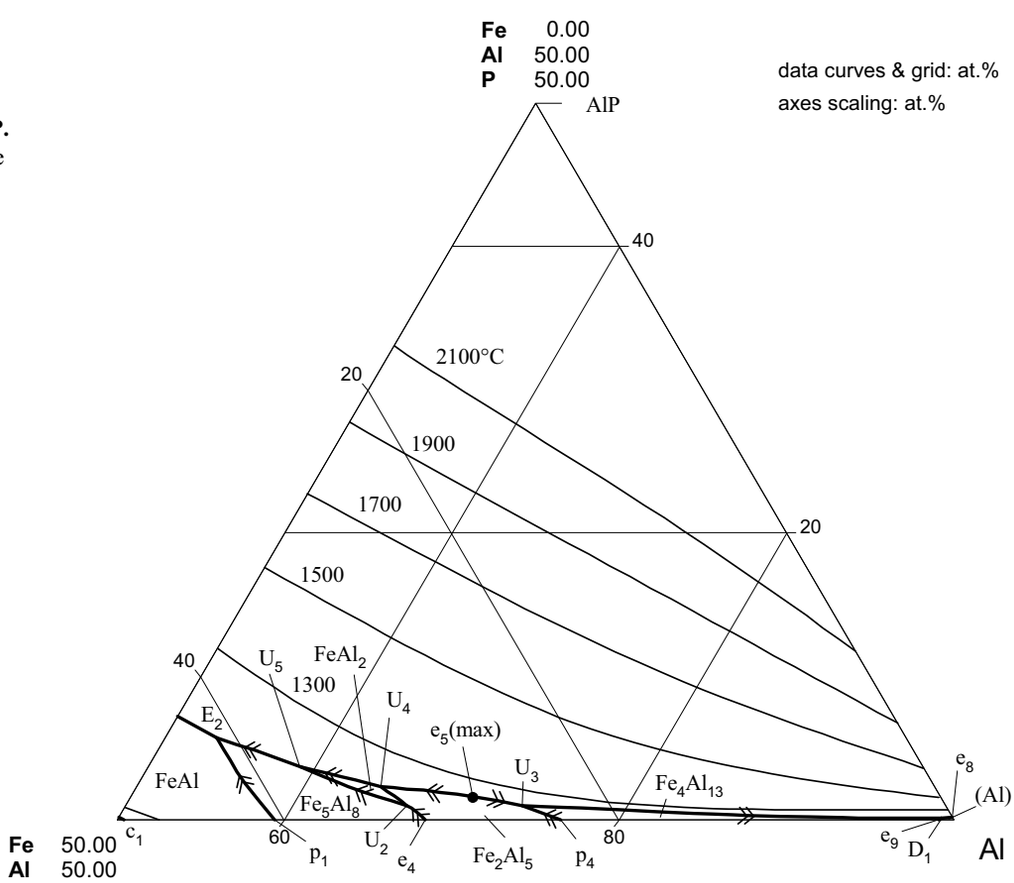

Fig. 2b: Al-Fe-P. Al rich part of the liquidus surface projection

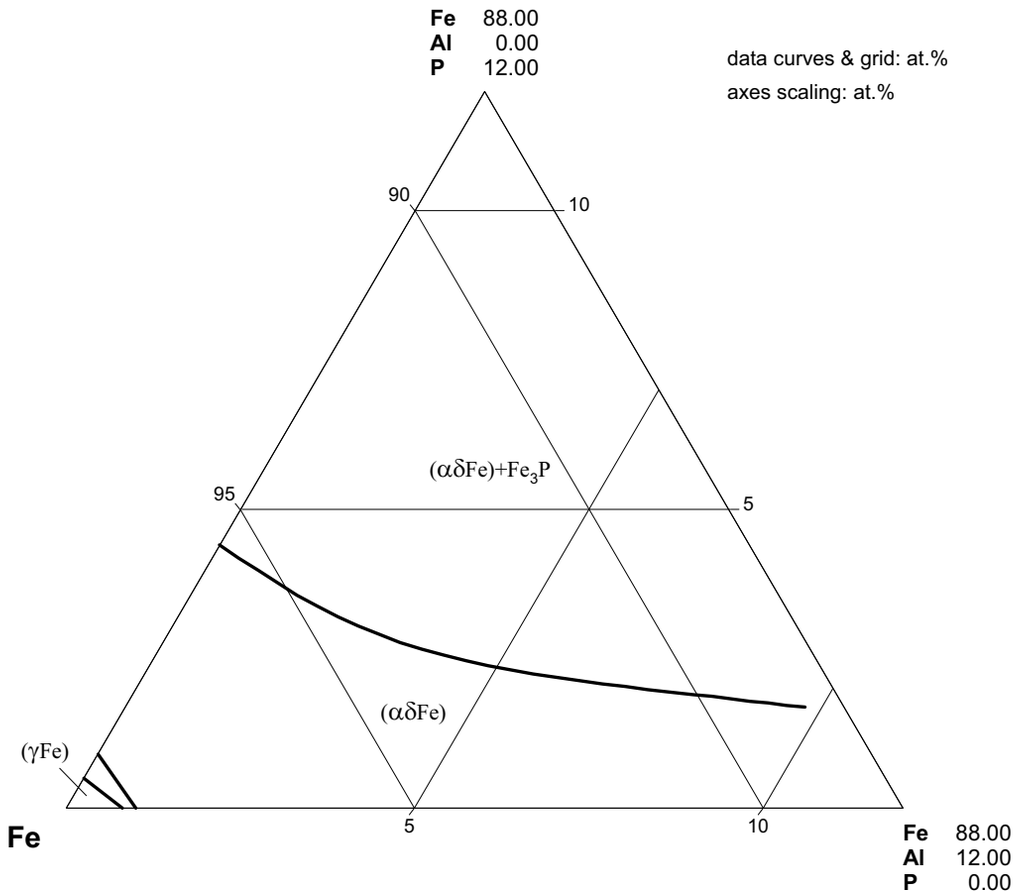

Fig. 3: Al-Fe-P.
Isothermal section in the Fe rich corner at 1000ºC

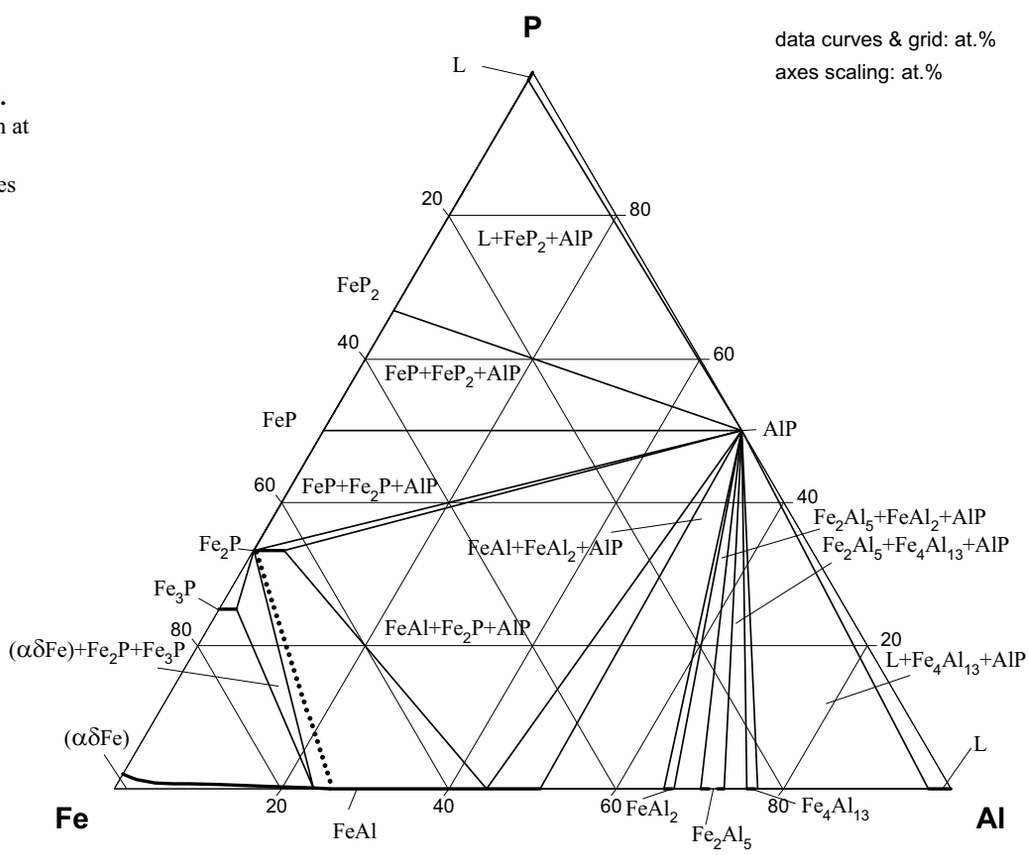

Fig. 4: Al-Fe-P.
Isothermal section at 800°C.
Dotted line denotes order-disorder transformation.

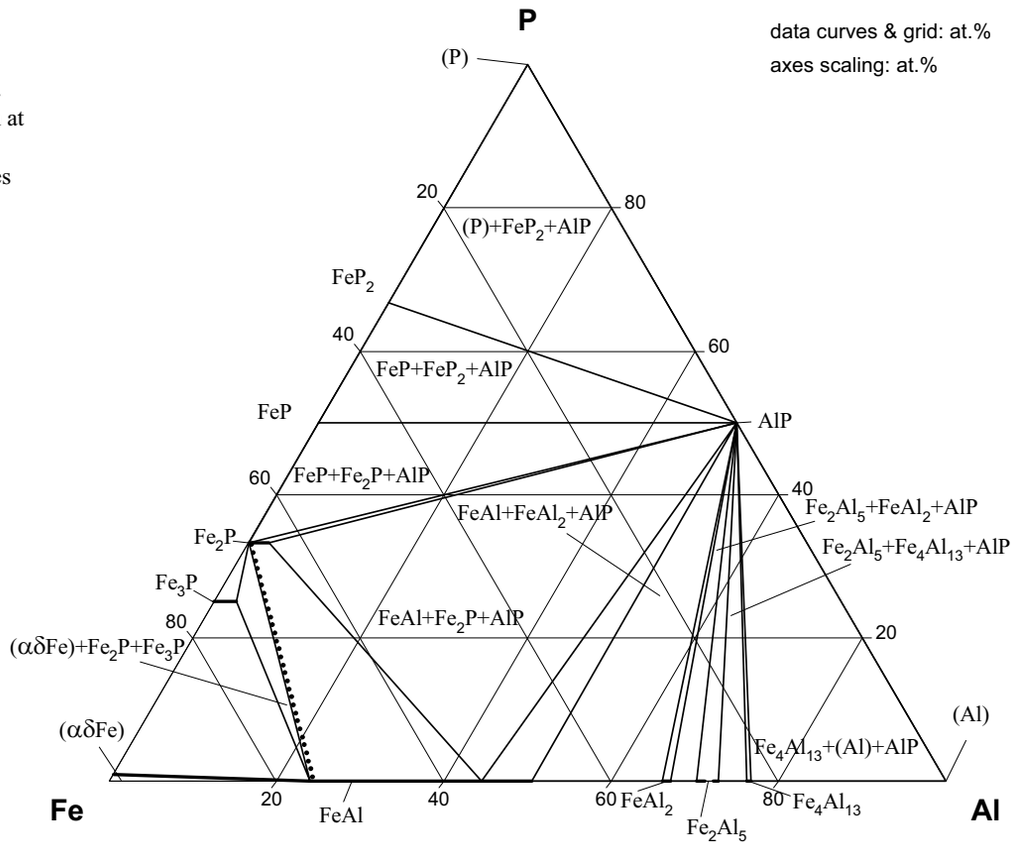

Fig. 5: Al-Fe-P.
Isothermal section at 650°C.
Dotted line denotes order-disorder transformation.

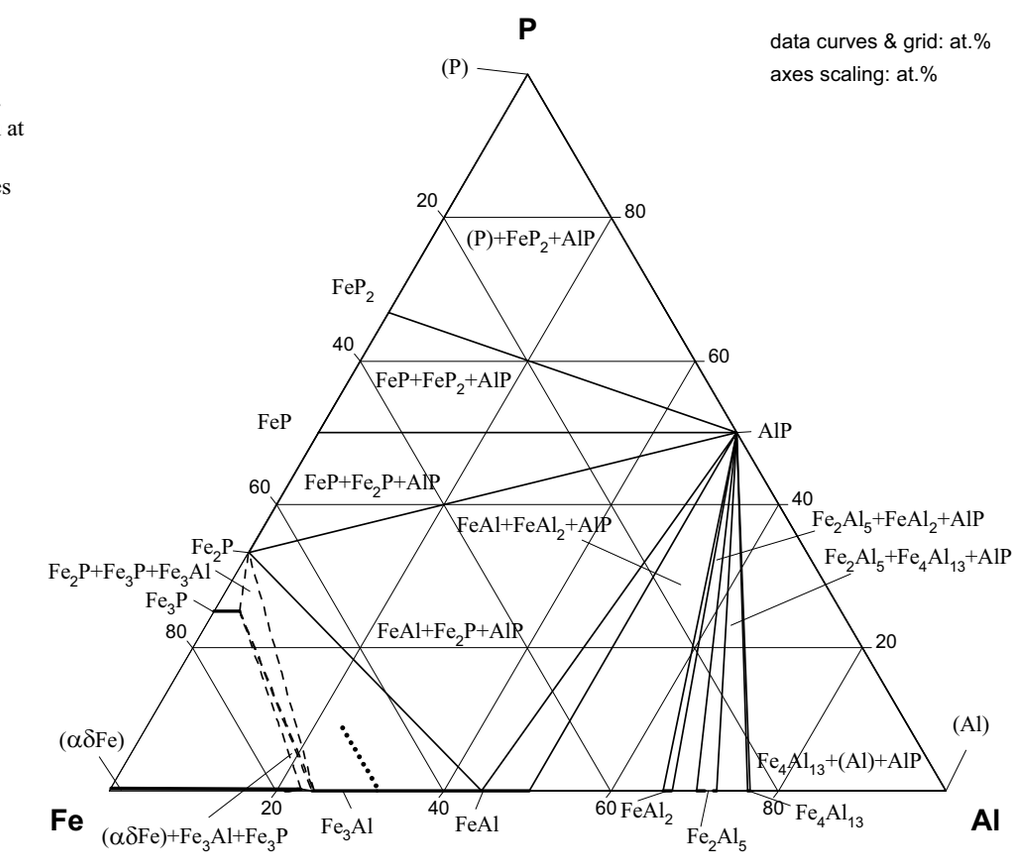

Fig. 6: Al-Fe-P.
Isothermal section at 450°C.
Dotted line denotes order-disorder transformation.

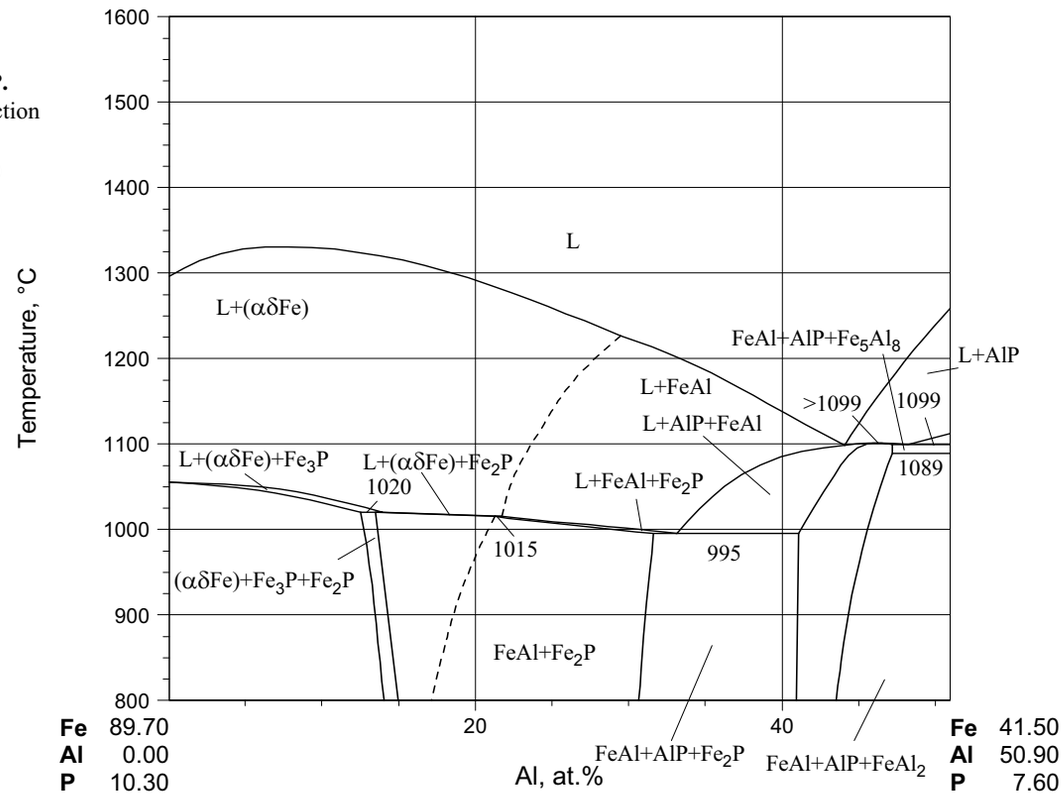

Fig. 7: Al-Fe-P.
Partial vertical section at 6 mass% P (redrawn in at.%)

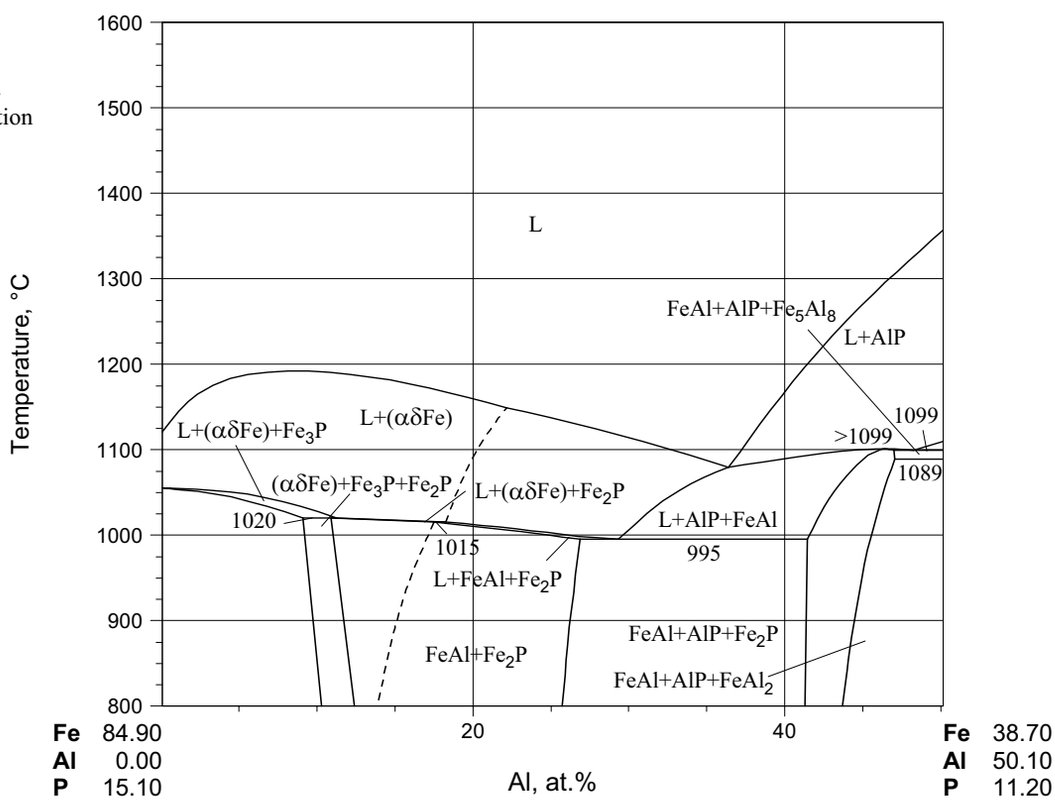

Fig. 8: Al-Fe-P.
Partial vertical section at 9 mass% P (redrawn in at.%)

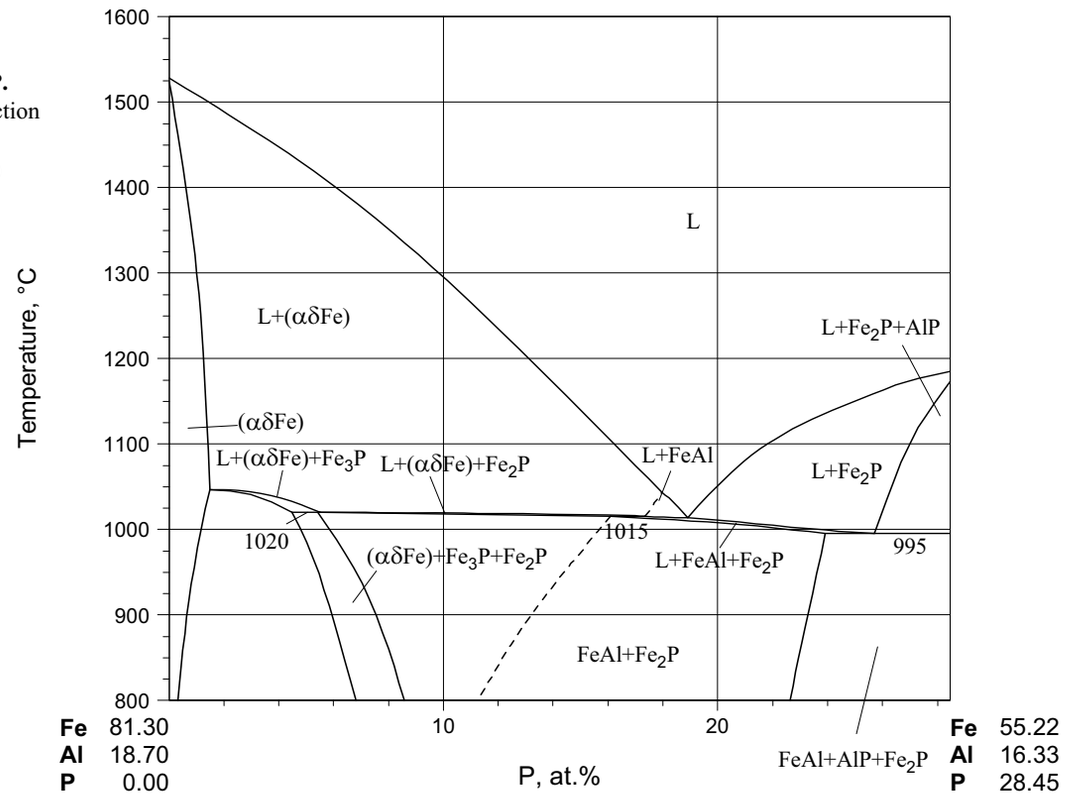

Fig. 9: Al-Fe-P.
Partial vertical section at 10 mass% Al (redrawn in at.%)

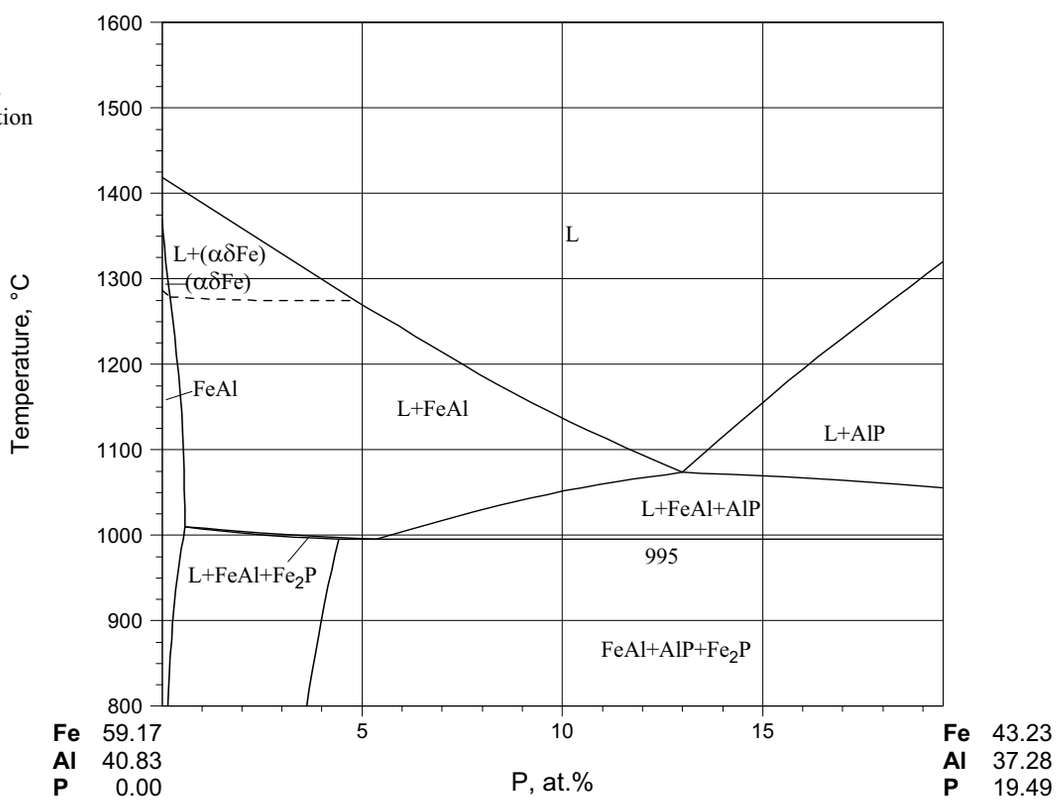

Fig. 10: Al-Fe-P.
Partial vertical section at 25 mass% Al (redrawn in at.%)

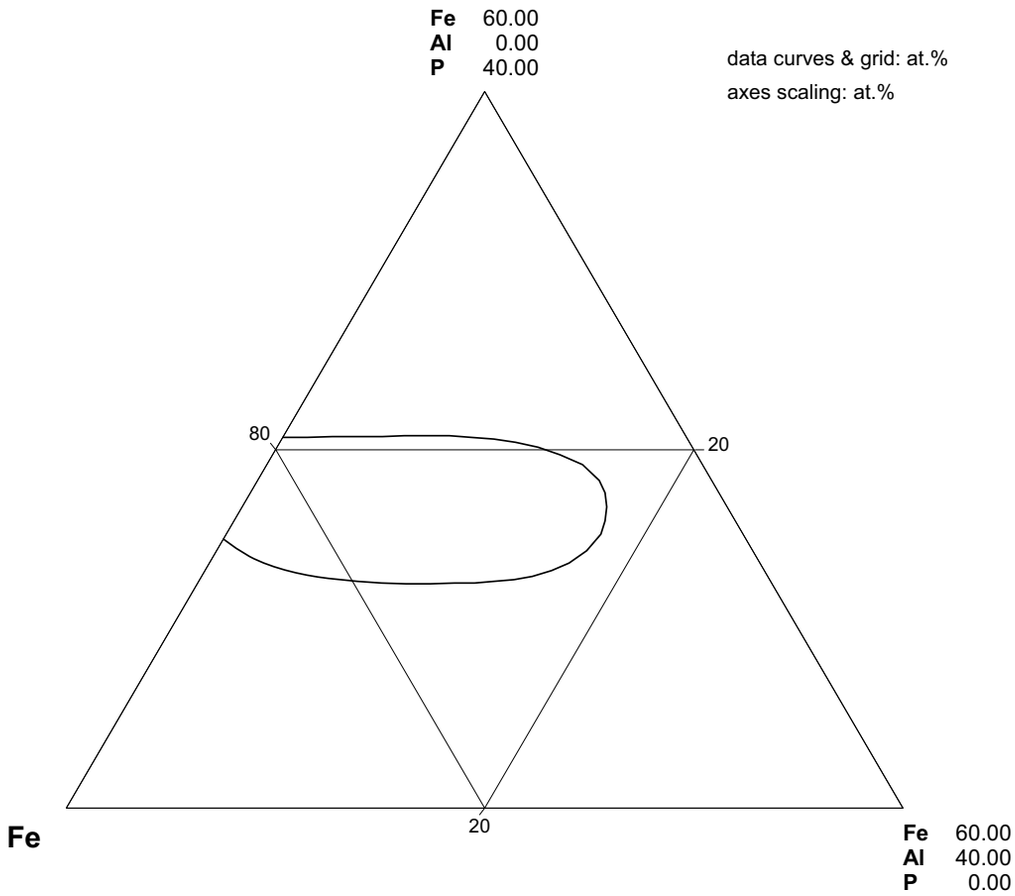

Fig. 11: Al-Fe-P.
Range of glass state